

## Long-Range Energy Transfer in Self-Assembled Quantum Dot-DNA Cascades

*Samuel M. Goodman,<sup>a</sup> Albert Siu,<sup>a</sup> Vivek Singh,<sup>a</sup> Prashant Nagpal<sup>a,b,c,d\*</sup>*

<sup>a</sup> *Department of Chemical and Biological Engineering, University of Colorado, Boulder*

<sup>b</sup> *Materials Science and Engineering, University of Colorado, Boulder*

<sup>c</sup> *BioFrontiers Institute, University of Colorado, Boulder*

<sup>d</sup> *Renewable and Sustainable Energy Institute, University of Colorado, Boulder*

<sup>\*</sup> *Corresponding Author: Email: pnagpal@colorado.edu*

### Supplementary Information

## SI – Materials and Synthesis

### **Synthesis Chemicals**

3-Mercaptopropionic acid ( $\geq 99\%$ ) was purchased from Acros Organics. Cadmium(II) chloride (technical grade), ammonium fluoride ( $\geq 98\%$ ), and hexamethylenetetramine ( $\geq 99.0\%$ ) were purchased from Sigma Aldrich. Tellurium -325 mesh powder (99.99% metal basis) was purchased from Alfa Aesar. Sodium borohydride (98%), sodium hydroxide ( $\geq 97.0\%$ ), and ethylene glycol (certified) were purchased from Fisher Scientific. Compressed nitrogen (pre-purified) and oxygen (ultrahigh purity) were purchased from Airgas. Ethanol (200 proof) was purchased from Decon Laboratories INC. DNA sequences were custom ordered from Integrated DNA Technologies. All purchased materials were used as provided without further purification.

### **DNA Sequences**

DNA sequences are labeled according to the position of the conjugated QD in a ternary complex L-M-O (L - largest dot, M - middle dot, O - outer dot), the number of possible connections with other dots (1 or 2), and which strand is complementary (for the outer dots). For example, a ternary complex consisting of a red dot, yellow dot, and green dot would be described as R(L1)-Y(M<sub>2</sub>)-G(O<sub>1</sub>M), while a central red dot connected to two green dots would be described as G(O<sub>1</sub>L)-R(L<sub>2</sub>)-G(O<sub>1</sub>L). A \* in a sequence refers to a phosphorothioate linkage which is the binding moiety for conjugation to the QD surface. In the case of L<sub>2</sub>, the 2 refers to the ability of the large QD to accommodate two different DNA strands.

L<sub>1</sub>: 5' – (G\*)<sub>20</sub> A<sub>10</sub> AAA GGA A – 3'

L<sub>2</sub>: 5' – (G\*)<sub>10</sub> A<sub>10</sub> AAA GGA A – 3'

M<sub>2</sub>: 5' – TCC GCT GCA G A<sub>10</sub> (G\*)<sub>17</sub> A<sub>10</sub> TTC CTT T – 3'

O<sub>1</sub>L: 5' – (G\*)<sub>10</sub> A<sub>10</sub> TTC CTT T – 3'

O<sub>1</sub>M: 5' – CTG CAG CGG A<sub>10</sub> A\* (G\*)<sub>9</sub> G – 3'

### **CdTe Quantum Dot Synthesis**

Deionized water was initially degassed using bubbling nitrogen for 30 min. 1 mL degassed water was used to dissolve NaBH<sub>4</sub> (35 mg, 0.93 mmol), and the resulting solution was transferred to a septum-capped 2 mL vial (Thermo Scientific) containing Te powder (40 mg, 0.31 mmol). A needle was inserted into the septum for outgassing during the reaction, which was allowed to proceed until the tellurium precursor solution became optically clear and colorless. A cadmium precursor solution was created by dissolving CdCl<sub>2</sub> (3.7 mg, 0.020 mmol) and 3-mercaptopropionic acid (1.8  $\mu$ L, 2.2 mg, 0.021 mmol) in 10 mL of degassed water. The reaction solution was made by mixing 250  $\mu$ L of the cadmium precursor solution, 200  $\mu$ L degassed

water, 1  $\mu\text{L}$  of the tellurium precursor solution, 10  $\mu\text{L}$  of 0.5 M NaOH, and 50  $\mu\text{L}$  of 1 mM DNA solution (total volume 511  $\mu\text{L}$ ). 100  $\mu\text{L}$  aliquots of the reaction solutions were divided into 5 PCR tubes (Life Science Products INC), and placed in a PCR machine (Applied Biosystems GeneAmp PCR System 9700). The tubes were held at 98°C for the reaction duration. The quantum dots were then filtered (Omega 30K Nanosep OD030C33), and washed with pH 10 water. The purified dots were re-dispersed in 150  $\mu\text{L}$  pH 10 water for storage. Quantum dots without DNA were synthesized in the same manner, replacing the 50  $\mu\text{L}$  DNA solution with 50  $\mu\text{L}$  degassed water. DNA conjugated QDs exhibited long term stability over several months while non-DNA conjugated QDs became non-luminescent within several weeks. See figure S1 for size distribution histograms of the CdTe dots determined by TEM.

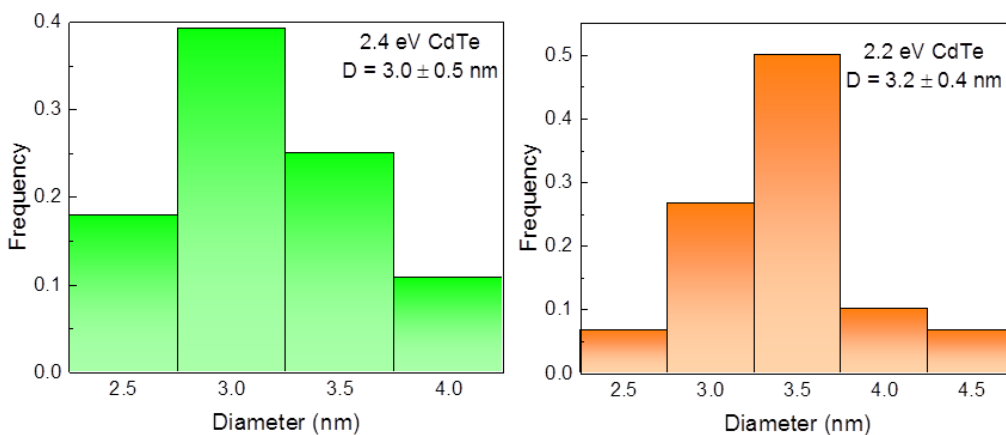


**Figure S1** – Size distribution histograms of green and red emitting CdTe quantum dots.

## Complex Formation

QD complexes were formed by mixing dots with complementary DNA strands in a stoichiometric ratio, and heating the mixture to 70°C for 1 h in the PCR machine. QD concentrations were determined from optical absorption as described in Yu et al.<sup>15</sup>

## TiO<sub>2</sub> Substrates

TiO<sub>2</sub> nanotubes were grown via anodization in a solution of ethylene glycol containing 1wt% NH<sub>4</sub>F at room temperature.<sup>21</sup> A titanium sheet, cut to desired dimensions, served as the anode and a platinum electrode as the cathode. The voltage was kept at 30 V by a DC power supply throughout the etching process. Nanotubes between 4-8  $\mu\text{m}$  served as substrates in the device experiments.

## Sensitizing TiO<sub>2</sub> Substrates with Quantum Dots

Substrates were initially sensitized by exposure to ozone plasma for 10 min. They were then immersed in 400  $\mu\text{L}$  of the stock QD solution such that the liquid level was 10 mm above the bottom of the substrate. The solution was then heated in a temperature controlled oil bath at 70°C for one hour. The substrate was then removed from the QD solution and rinsed with 200  $\mu\text{L}$  pH 10 water. Successive sizes were added by immersing the sensitized substrate in a solution of the next QD to form the desired sequence, and repeating the above procedure.

## SII – Optical, Single Particle, and Electrical Characterization

### Optical Spectroscopy

UV-VIS spectra were acquired on a Beckman Coulter DU 730 at 1 nm resolution. Photoluminescence spectra were measured by illuminating the sample with a UV lamp (UVP UVGL-25) and collecting the resulting emission spectrum with an Ocean Optics USB 4000 detector. A photo of the solutions measured in Figure 1c is shown in Figure S2.

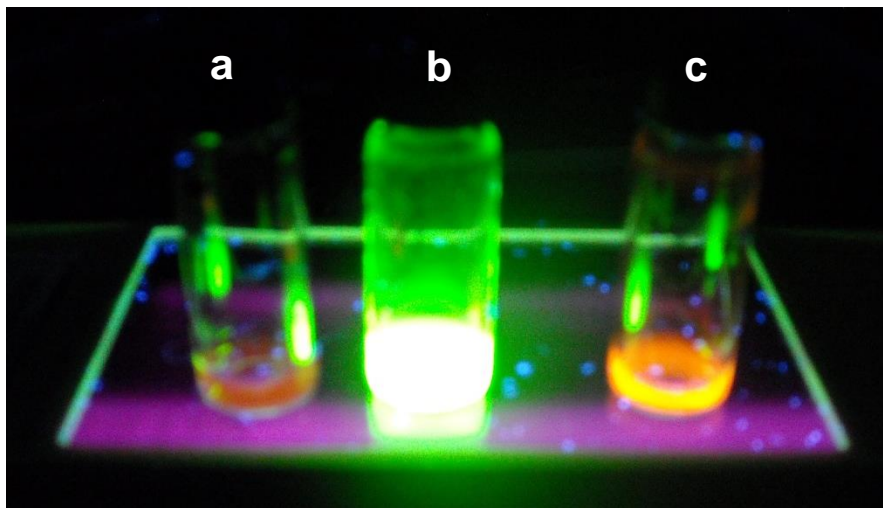


**Figure S2** – Photoluminescence of solutions of (a) orange dots with DNA, (b) green dots with DNA, and (c) a G<sub>2</sub>O complex exhibiting enhanced orange emission. The complex concentration is half of the solely orange solution.

### Transmission Electron Microscopy

TEM images were obtained by the CAMCOR facility at the University of Oregon, and with a Philips CM 100 at 80 kV (Figure S3).

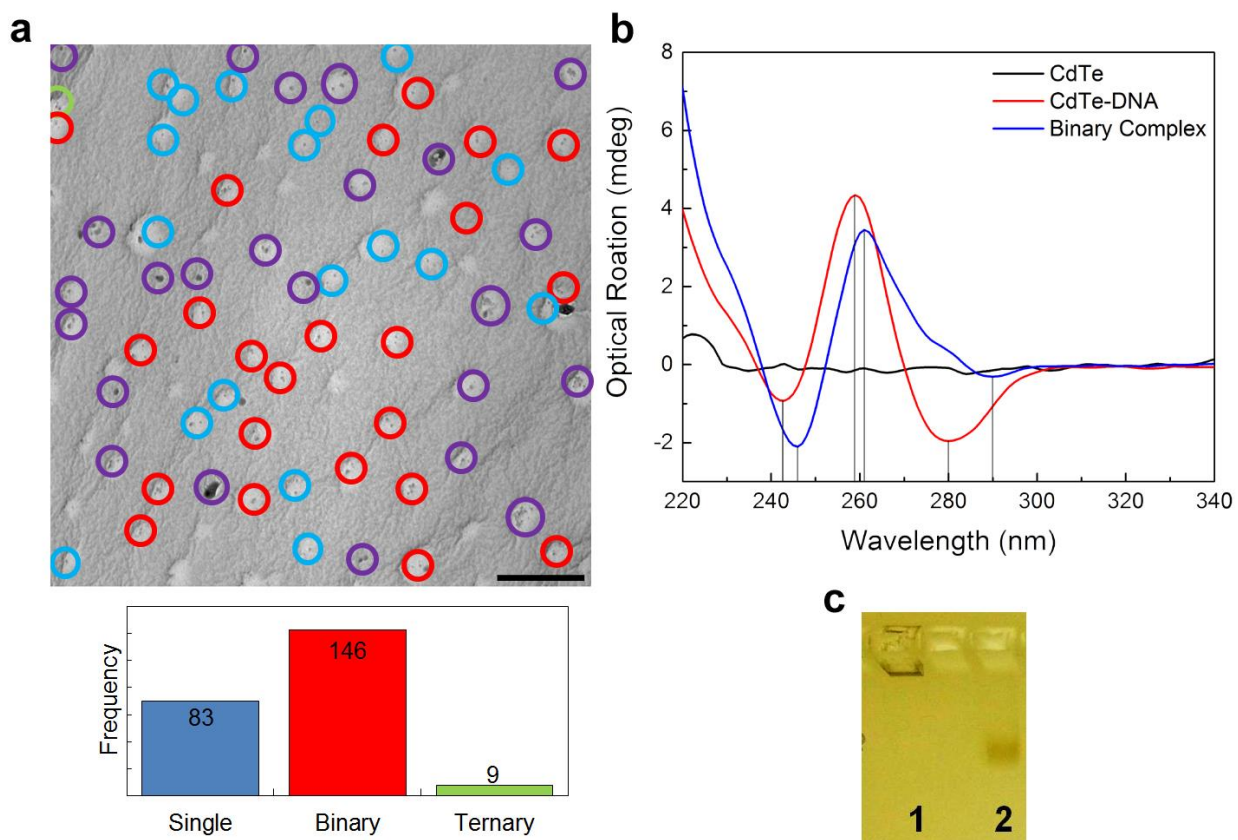


**Figure S3** – (a) Low magnification TEM image of a sample of yellow-red binary complexes (scale bar is 500 nm) with binary complexes circled in red, ternary complexes circled in green, and unbound dots circled in blue. A histogram showing the total number of dots in each configuration is included below the image. The total number of observed dots in each configuration is included with the histogram. Ambiguous features not counted in the analysis are circled in purple. (b) Circular dichroism spectrum of CdTe quantum dots without DNA, CdTe as synthesized with single stranded DNA, and binary complexes exhibiting spectrum shifts due to the hybridization of the binding sections (handedness of the hybridized ds-DNA can be clearly seen, Kyper et. al., *Nucleic Acid Research* **2009**, 37, 1713-1725; and Suga et. al., *Nucleic Acid Research* **2011**, 39, 8891-8900). Shifts in feature positions post-hybridization are marked. (c) Photograph of an agarose gel plate showing how to separate particles with (2) and without (1) DNA, the same principle holding for complexed and un-complexed quantum dots.

### Definition of Photoresponse

The parameter called photoresponse ( $R$ ) used in Figures 3 and 4 is defined using equation S1. First, the measured dark current ( $I_{dark}$ ) is subtracted from the light current ( $I_{\lambda}$ ) to calculate the absolute value of the photocurrent of the specific dot or complex at a certain wavelength ( $\lambda$ ). This photocurrent is normalized by the light intensity at that wavelength output by the lamp as measured by a calibrated Newport power meter to allow quantitative comparison of the different energy peaks.

$$R = \frac{I_{\lambda} - I_{dark}}{P_{\lambda}} \quad (S1)$$

### Current Sensing Atomic Force Microscopy

CS-AFM measurements were taken using gold coated (5 nm Cr / 15 nm Au, in house, Figure S4 plasmon absorbance) silicon AFM tips (NanoDevices INC). Dilutes samples were drop cast on ITO substrates, which allowed illumination with monochromatic light to measure the photoresponse, with wavelength controlled by a Princeton Instruments Action SP2150 monochromator with filters to remove 2<sup>nd</sup> order diffraction (Thor Labs 315-710 nm Band Pass filter). Light intensity was measured by a Newport Power Meter Model 1918-R after each set of measurements. Individual complexes were located in soft contact mode to avoid perturbing their separation (see Figure S5 for representative images). The average distance between particles was measured as  $6 \pm 2$  nm (theoretical maximum of 9.7 nm assuming 3.6 Å separation between individual bases).

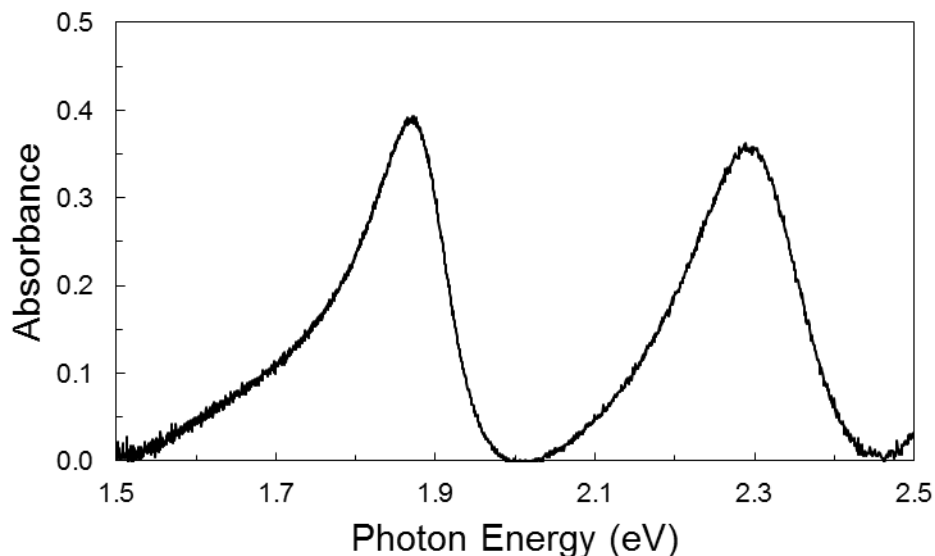


**Figure S4** – Plasmon absorbance spectra of the gold-coated CS-AFM tips.

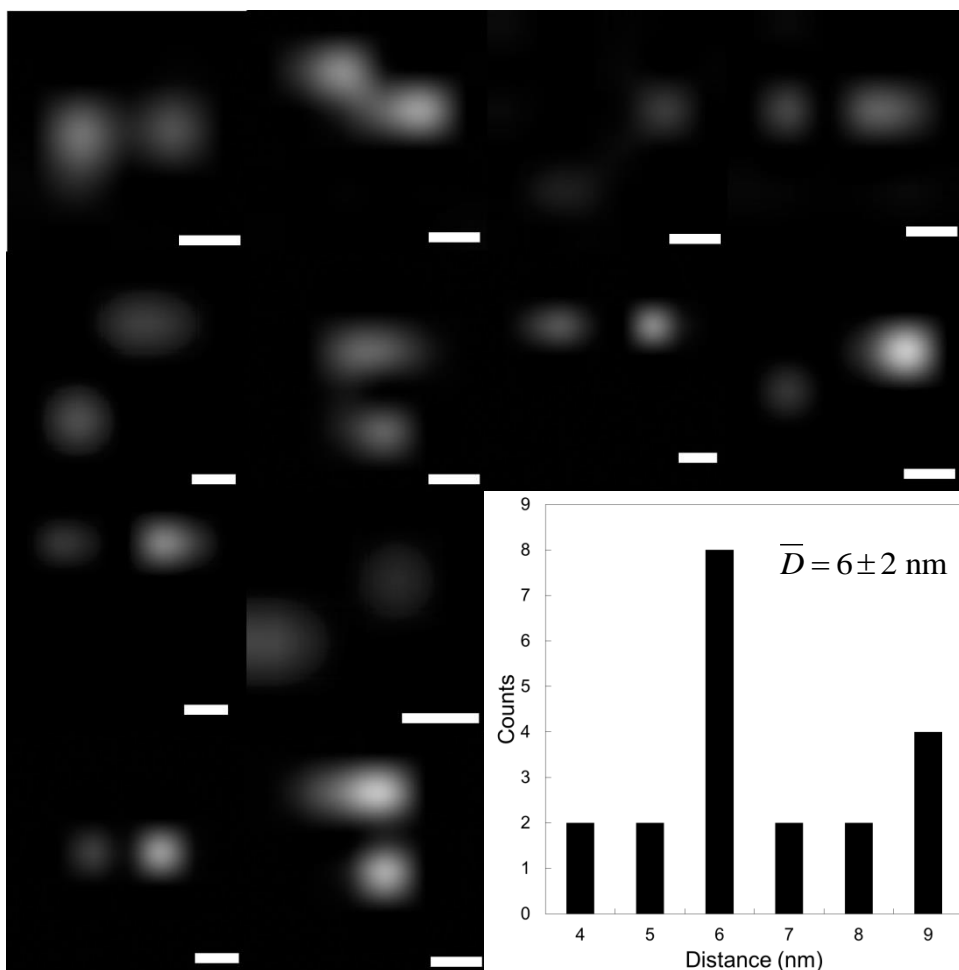


**Figure S5** – Complexes as seen by CS-AFM (scale bars are 5 nm). Histogram showing the distribution of interparticle distances for 20 independent complexes is included.

The I-V curves were analyzed in order to determine the likely charge transport mechanism, and were found to conform to Schottky emission (equation S2, Figure S6). Based on these fits we were able to calculate the residual ( $r$ , equation S3) at each point to estimate the error of the photocurrent. For example, for the curves shown in Figure 3a, the 590 nm photocurrent ( $I_{\lambda} - I_{dark}$ ) has a value of  $1.09 \pm 0.06$  nA (equation S4) while the 539 nm photocurrent has a value of  $4.3 \pm 0.3$  nA at 700 mV, implying the photoresponse will have an uncertainty of ~5-7% (the light power measurement is an order of magnitude more precise and will not be a dominant contributor to the photoresponse error). Repeating this calculation using the average of all residuals ( $\bar{r}$ ) for each curve predicts an uncertainty of ~3-5%.

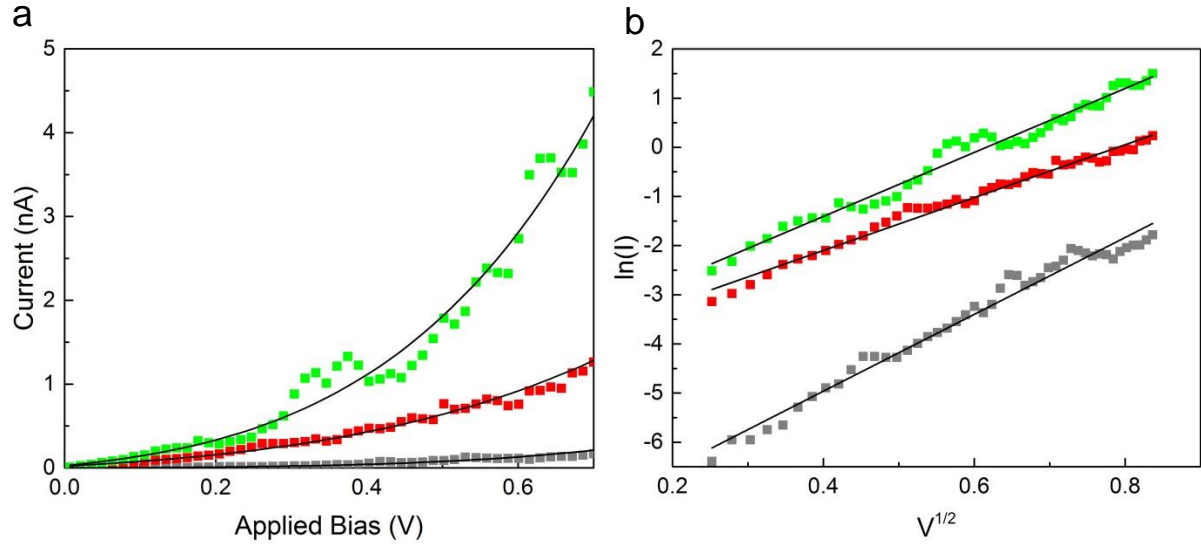


**Figure S6** – Fits of the measured I-V curves to Schottky emission (a) and the linearized forms used to fit the data (b).

$$I \propto T^2 \exp \left[ -\frac{q}{kT} \left( \phi - V^{1/2} \sqrt{\frac{q}{4\pi\epsilon}} \right) \right] \quad (\text{S2})$$

$$r = |I_{\text{measured}} - I_{\text{fit}}| \quad (\text{S3})$$

$$\sigma_R = r_{I_\lambda} + r_{I_{\text{dark}}} \quad (\text{S4})$$

### Low Temperature Measurements

Devices were measured in an Advanced Research Systems vacuum cryostat chamber (DE202AE with an ARS-2HW compressor) with temperature controlled by a Lakeshore 335 Temperature Controller. Current-voltage curves were measured with a Keithley 2612A System SourceMeter. A tungsten lamp (GE 35200-EKE) provided sample illumination with wavelength controlled by a monochromator with filters to remove 2<sup>nd</sup> order wavelengths. Light intensity was recorded after each set of measurements. Dark Measurements were taken first, with five replicates each. When measuring each wavelength the device was exposed to the light for five seconds before measuring the I-V curves. Each I-V curve consists of 101 total points with a scan rate of 50 ms per point. After taking each I-V curve the light beam was blocked by placing a physical barrier between the device and monochromator. I-V curves within the standard error of the dark measurements were treated as having zero response. See Figure S7 for a schematic of the measurement apparatus and images of QD-decorated nanotubes.



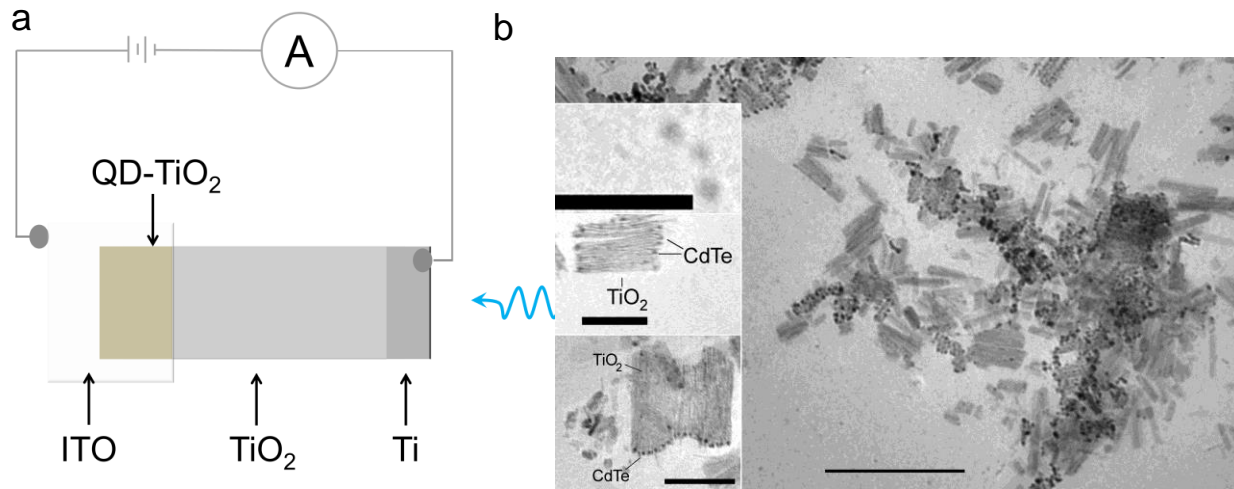


**Figure S7** – (a) Schematic of device measurements. A portion of the  $\text{TiO}_2$  substrate is sensitized with QDs ( $\text{QD-TiO}_2$ ) while another portion is scraped clean to make an Ohmic contact (Ti). An ITO coated class slide serves as the second electrode, which allows illumination for photoresponse measurements. Each electrode is connected to a sourcemeter which measures the I-V characteristics. (b) TEM images of nanotubes scraped from the surface of the titanium substrate showing nanoparticle decoration (500 nm scalebar). Inset images from top to bottom are a single ternary complex (50 nm scalebar), and two sections of nanotubes showing primary nanoparticle attachment to the termini (100 nm scalebars).

### SIII – Energy Transfer Model

Energy transfer in the binary quantum dots complexes was modeled according to Förster FRET. The value of the integral in eq. 1 is visualized in Figure S8. The variances were calculated using eq. S5 and the CS-AFM peak data.  $F_D$  and  $\varepsilon_A$  were converted from eV to functions of wavelength ( $\lambda$ ) prior to integration (eq. S7). The Stoke's shift ( $\Delta E_S$ ) was assumed to be constant for single particles and bulk (Figure 1b).

$$\sigma = FWHM [8\ln(2)]^{-1/2} \quad (\text{S5})$$

$$E(\text{eV}) \times \lambda(\text{nm}) = 1239.8(\text{eV} \cdot \text{nm}) \quad (\text{S6})$$

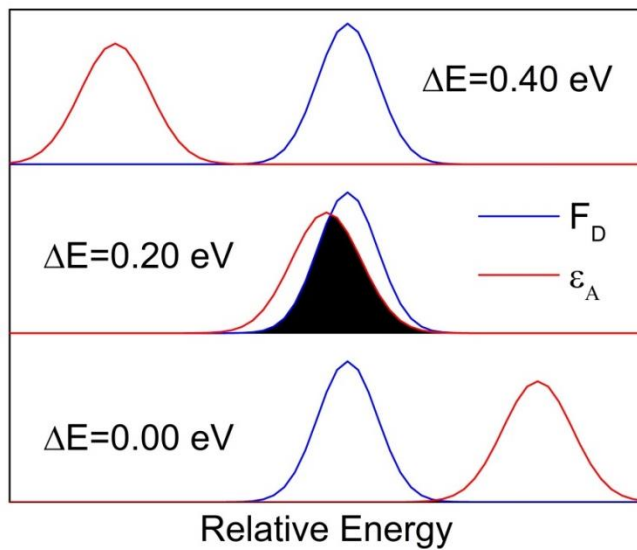


**Figure S8** – First excitonic wavefunction convolutions (filled black) across the modeled range.